RSC Advances

ROYAL SOCIETY OF CHEMISTRY

www.rsc.org/advances

Cite this: DOI: 10.1039/c0xx00000x

www.rsc.org/xxxxxx

Paper

The influence of Formaldehyde/Phenol Molar Ratio on Microstructure of B-OMCs

Jing Song, Yan Zhang*, Yujian Liu

Received (in XXX, XXX) Xth XXXXXXXXX 20XX, Accepted Xth XXXXXXXXX 20XX

DOI: 10.1039/b000000x

Boron-doped ordered mesoporous carbons (B-OMCs) were prepared via solvent evaporation induced self-assembly (EISA) method by using triblock copolymer (Pluronic F127) as a soft template, boron modified phenolic resins as both boron and carbon precursors. The effect of molar ratio of formaldehyde to phenol (F/P) on the microstructure and character of B-OMCs was especially investigated. The results show that the specific surface area of B-OMCs increases along with the increase of F/P, while pore size and boron content of B-OMCs increase at first, then drop off. The material prepared with F/P=1.5/1 possesses best-ordered mesostructure, higher specific surface area (667 m^2/g), larger pore size (7.9 nm), and highest boron content (1.26 wt%). And it also exhibits superior electrochemical performances and high specific capacitance (180 F/g).

1. Introduction

Since the first mesoporous carbon material (CMK-1) was reported in 1999 by Ryoo et al.,[1] ordered mesoporous carbons (OMCs) have attracted much attention due to their excellent physical and chemical properties and potential applications in many aspects.[2-4] OMCs with different structures and various morphologies have been prepared.[5,6] In recent years, heteroatoms, such as boron,[7,8] nitrogen[9,10] and phosphorus[11,12] have been adopted to improve the properties of OMCs, which can broaden their applications ranging from catalysis to hydrogen and energy storage.[13-16] Boron with three valence electrons, shifts the Fermi band downwards by substituting for carbon at the trigonal sites, and tunes the properties of oxygen chemisorption and electrochemistry for redox reactions.[17,18] It was shown that the boron doping may improve the specific capacitance per unit surface area for the carbon materials[19] and that boron-containing mesoporous carbons show a higher capacitance (~1.6 times) than that observed for carbons without boron in aqueous electrolyte solutions.[7]

Many approaches have been tried to fabricate boron-doped mesoporous carbon (B-OMC), such as nanocasting,[7] sol-gel,[20] self-assembly,[16] etc. Da-wei Wang[7] obtained boron-containing mesoporous carbons by using SBA-15 as hard template, sucrose as carbon precursor and boric acid as boron precursor, but B-OMCs with only 0.16 wt% boron content was achieved. Boron and phosphorus doped mesoporous carbons were also synthesized by using a soft-templating method.[16] However, the resultant materials have maximum boron doping of only about 0.97 wt% and average pore width in the range between 4.9 and 5.4 nm. The main reason for very low doping boron content is that during preparation boron is just physically mixed into the precursors, so that it is apt to volatilize at the temperature over 500 °C and too much boron atoms would also disturb the formation of well order mesoporous. Nevertheless, in most potential utilization, especially for supercapacitors, B-OMCs should have a high specific surface area, large pore size and well developed mesoporosity.[8] As boron modified phenolic resin (BPF), owing to its better thermal stability, is a good boron and carbon precursor, a little research work is trying to use boron modified phenolic resins as the precursor of B-OMCs. Zhai[21] prepared B-OMCs with BPF via organic-inorganic co-assembly, while the maximum boron content of B-OMCs is only 0.33 wt%. Her other study[22] raised boron mass fraction of B-OMCs to 1.12 wt%, but just getting small specific surface area (277 m^2/g). By using BPF, Zhao[23] successfully prepared B-OMC with boron content varying from 0.67 to 1.64 wt%, but when the boron content over 1.01 wt%, its specific surface area decrease greatly (from 462 to 314 m^2/g). It seems that B-OMCs both with high boron content and ideal order mesoporous structure are not easy to be obtained.

There are several key requirements for the successful synthesis of mesoporous carbon materials using soft templates,[5] such as the ability of the precursor components to self-assemble into nanostructures, the stability of the pore-forming component and the ability of the carbon-yielding component to form a highly cross-linked polymeric material. The choice of resol as a precursor, a kind of carbon-yielding component, is critical to the successful organization of organic-organic mesostructures

*Key Laboratory of Specially Functional Polymeric Materials and Related Technology, Ministry of Education, School of Materials Science and Engineering, East China University of Science and Technology, MeiLong Road 130, Shanghai 200237, PR China.

E-mail address: yzhang@ecust.edu.cn (Y. Zhang); fax: +86 21 64252659

Tel.: +86 21 64252394

because resol has a large number of hydroxy groups (-OH) which can interact strongly with triblock copolymers through formation of hydrogen bonds.[24,25] It is generally believed that resols with molecular weight in the range of 200-5000 are all suitable precursors for the synthesis of the ordered mesostructures.[26] Little attention has been paid to the impact of phenolic resin itself on the property of OMCs. However, boric acid would react with some hydroxymethyl groups of phenolic resins, which would weaken hydrogen bond action of resins and templates in the process of self-assembly. And with the molecular weight of BPF rising, its poor solubility in ethanol would also interfere EISA process.

Periodical pore structure formed by using soft template method depends on both polymerization of phenolic resins and their self-assembly process. The molar ratio of formaldehyde to phenol exercises a key influence on the structure of the phenolic resin network, its curing reaction and subsequent carbonization behaviour, especially for the self-assembly process and the property of B-OMC. However, little research has been undertaken in this field yet. In this paper, the effect of molar ratio of F/P on the mesostructure of B-OMCs in EISA route is investigated extensively. Besides, electrochemical performances of the resulting B-OMCs are further studied.

2. Experimental

2.1 Chemicals

Poly(ethylene oxide)-poly(propylene oxide)-poly(ethylene oxide) triblock copolymer ($EO_{106}PO_{70}EO_{106}$, Pluronic F127) was acquired from Sigma-Aldrich, with an average molecular weight of 12600. Phenol, formaldehyde (37 wt%) and boric acid were purchased from Sinopharm Chemical Reagent Co., Ltd. All the reagents were used as received without further purification. Deionized water was used in all experiments.

2.2 Synthesis of boron modified phenolic resins (BPFs)

Boron modified phenolic resins were prepared as shown in Scheme 1. A low-molecular-weight phenolic resin was synthesized by mixing 18.8 g phenol, 19.5 g formaldehyde (37 wt%) and sodium hydroxide aqueous solution together in a flask, and stirring at 75 °C for 60 min. Then 20 g boric acid solution was added to the mixture and stirred for 30 min, while water was removed under vacuum. The final product was dissolved in ethanol for further use. The obtained boron modified phenolic resin was denoted as BPF-x, in which x represents the molar ratio of F/P, with the same amount of boric acid used.

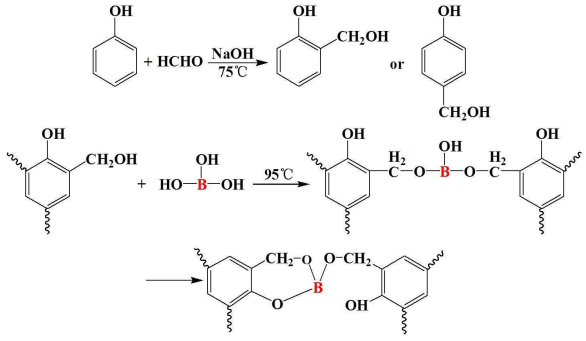

Scheme 1. Synthesis reaction of boron modified phenolic resin.

2.3 Synthesis of boron-doped mesoporous carbons (B-OMCs)

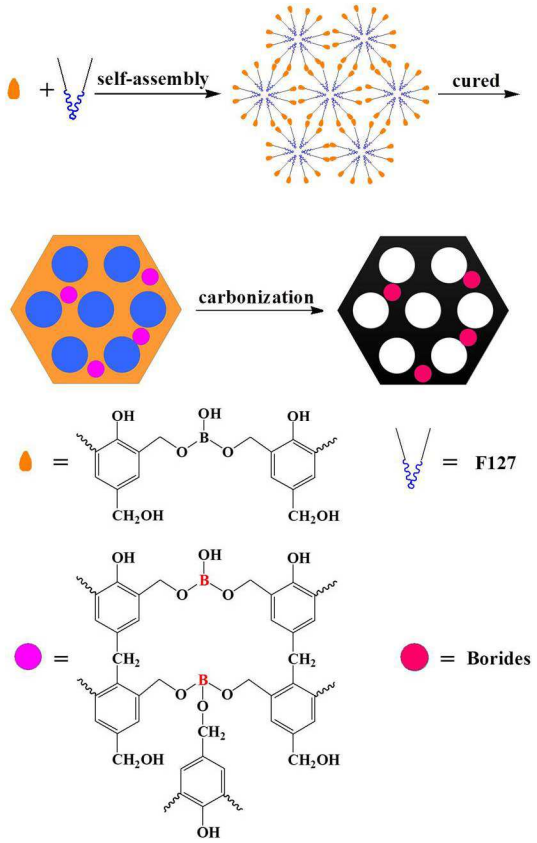

Scheme 2. A soft-templating route used for the synthesis of boron-doped ordered mesoporous carbon (B-OMC) using boron modified phenolic resin as precursor, triblock copolymer Pluronic F127 as a soft template.

B-OMCs were prepared via EISA method[24] by using boron modified phenolic resins obtained above as precursors (see Scheme 2). The poly(ethylene oxide)-poly(propylene oxide)-poly(ethylene oxide) triblock copolymer (Pluronic F127) was dissolved in ethanol, then BPF-x solution was added during stirring to form a homogeneous solution. Then it was poured into a dish to evaporate ethanol entirely at room temperature, followed by heating in an oven at 100 °C for 24 h to thermopolymerize the boron modified phenolic resin. Then the well-cured transparent film was scraped and calcined under nitrogen atmosphere at 350 °C for 2 h to remove the surfactant and followed by carbonization at 600 °C for 2 h, at a temperature increase rate of 1°C min^{-1}. The final product was denoted as B-OMC-x, with x representing the molar ratio of F/P.

2.4 Characterizations

Fourier transform infrared (FT-IR) spectra were collected on a Nicolet 5700 spectrometer. Boron modified phenolic resins were analyzed with further purification to remove unreacted boric acid. Powder X-ray diffraction (XRD) patterns were recorded on Rigaku D/max-2550 diffractometer using Cu-Kα radiation. Nitrogen adsorption-desorption measurements were performed at 77 K with a Micromeritics ASAP 2010 instrument. The BET

surface area and pore size distribution of samples were calculated with BET method and N_2 adsorption isotherm data. Transmission electron microscopy (TEM) images were obtained on a JEM-1400 instrument. X-ray photoelectron spectroscopy (XPS) was conducted on ESCALAB 250 equipped with Al-Kα radiation.

2.5 Electrochemical measurements

For preparing a working electrode, a mixture of an active material, acetylene black and poly(tetrafluoroethylene) (PTFE) with a weight ratio of 85:10:5 was homogenized in a mortar and pestle. Then the mixture was rolled into a thin film of uniform thickness (ca 60 μm), and punched into pellets with a diameter of 1 cm. Each active material was dried overnight at 110 °C, and the electrodes were impregnated with electrolyte under vacuum for several hours prior to the electrochemical tests. The tests were carried out in a Teflon Swagelok type two-electrode configuration, which was constructed with two facing carbon electrodes, sandwiched with a separator and a 3 M H_2SO_4 solution as the electrolyte.

The cyclic voltammetry (CV) tests were conducted using a PCI-4/300 potentiostat (Gamry, USA) in a potential range of 0-0.9 V. The galvanostatic charge-discharge (GC) measurements were conducted on the Arbin BT2000 apparatus. The gravimetric capacitance of electrode material was calculated according to the equation $C_m = 2I\Delta t / (m\Delta U)$, where I is the discharge current in ampere, Δt is the discharge time in second, m is the mass of active material on an electrode in gram, and ΔU is the working voltage in volt. In some cases, C_s is presented as F/m^2, which is obtained according to the equation $C_s = C_m / S_{BET}$.

3 Results and discussion

A comparsion of FT-IR spectra of the unmodified phenolic resin and the obtained resin is displayed in Fig.1 (a and b). The characteristic peaks at 1611 cm^{-1} and 1594 cm^{-1} are the skeleton vibration absorption of carbon-carbon double bonds (C=C) of benzen rings. The peaks at 887 cm^{-1}, 825 cm^{-1}, 757 cm^{-1} are owing to the C-H flexural of benzen rings. Those are characteristic absorption peaks of phenolic resin. Compared with the unmodified phenolic resin (curve a), a new absorption band at 1361 cm^{-1} corresponding to the B-O bond appears (curve b).[27] It means that the boron element is introduced into the backbone of the phenolic resin.

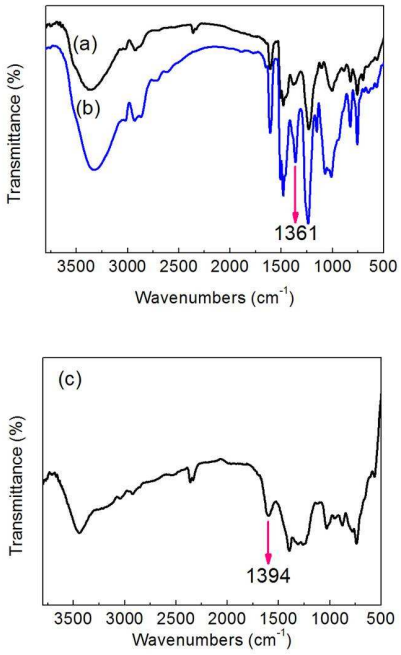

Fig.1 FT-IR spectra of unmodified PF (a), BPF (b) and B-OMC (c)

After carbonization, all absorption bands of B-OMC became rare and weak (Figure 1c). The absorption characteristic peaks at 1394 cm^{-1} should be corresponding to stretching vibration of triangular structure $[BO_3]$,[28] which indicates boron atoms are well preserved in the B-OMC.

The small-angle XRD (SAXRD) patterns of B-OMC samples prepared with different F/P ratio are shown in Figure 2. And the gel time of BPFs, structural parameters and boron contents of B-OMCs are summarized in Table 1. The diffraction peaks of B-OMCs at around 2θ=1° can be indexed as the reflection of ordered mesoporous structures. Although ordered structures were obtained, it is obvious that the diffraction intensity increases at first, and then decreases successively along with the increase of F/P. XRD patterns for B-OMC-1.5 and B-OMC-2.0 feature distinct peaks, indicating the presence of uniform and even ordered mesopores. As the major reactivity group in the phenolic resins, hydroxymethyl content rises with the augment of F/P. So the crosslink density of the phenolic resins as well as the thermal stability of carbon during pyrolysis increases with the rise of molar ratio of F/P. At the same time, the decrease of gel time indicates that the growth of molecular weight of the phenolic resin and the viscosity of the system. With the molecule getting larger, it will become more difficult for it to move freely and quickly in the self-assembly process for its larger steric hindrance. Self-assembly process would be disturbed, which leads to disordered mesoporosity. Therefore, BPF with either too low or too high polymerization degree is not suitable to prepare B-OMC with well-ordered mesoporous structure.

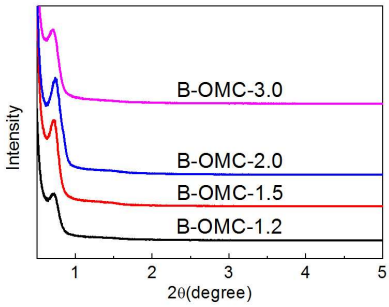

Fig.2 Small-angle XRD patterns of B-OMCs.

Figure 3 shows the TEM images of B-OMCs. Long 1D channels along the (100) direction as well as hexagonally arranged pores along the (001) direction (Fig.3b and d insets) can be clearly observed for all samples, indicating the ordered mesoporous structures. However, the order degree of B-OMC-1.2 seems to be inferior to that of B-OMC-1.5, which can be imputed to collapse of pore walls because of its poor structural stability during calcination (as shown in Fig. 3a and b). Besides, the spatial distribution regularity of B-OMC-3.0 is not as good as that

of other samples. These phenomena were consistent with the results of SAXRD patterns.

Table 1 Gel time of BPFs, structural parameters, B contents and specific capacitance of B-OMCs

Sample	t[a](s)	S_{BET}(m^2/g)	S_{micro}(m^2/g)	V_p(cm^3/g)	V_{micro}(cm^3/g)	D_p[b](nm)	$B_{cont.}$[c](wt%)	C[d](F/m^2)
B-OMC-1.2	145	610	278	0.65	0.15	7.8	1.10	0.21
B-OMC-1.5	122	667	274	0.72	0.15	7.9	1.26	0.27
B-OMC-2.0	107	687	291	0.71	0.16	6.9	1.22	0.25
B-OMC-3.0	81	691	307	0.72	0.17	7.0	1.19	0.23

[a] measured at 150°C.

[b] pore diameter, obtained from the maximum of the pore size distribution curve.

[c] determined by ICP.

[d] specific capacitance per surface area.

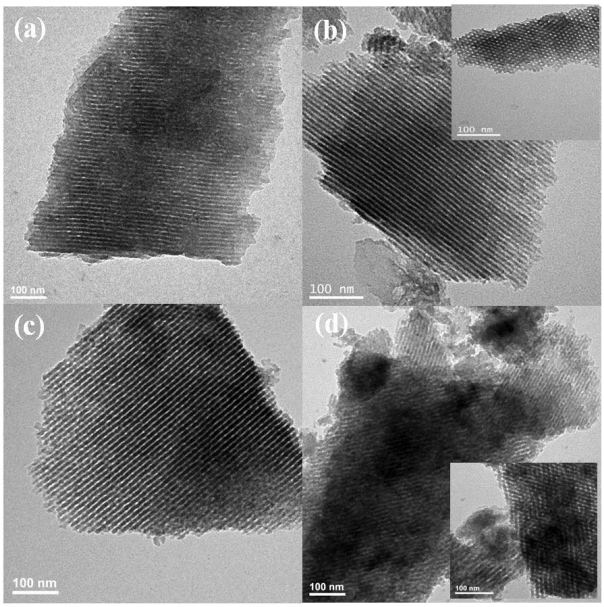

Fig.3 TEM images of B-OMC-1.2 (a), B-OMC-1.5 (b), B-OMC-2.0 (c), and B-OMC-3.0 (d).

The N_2 adsorption/desorption isotherms and pore size distribution curves of B-OMCs are presented in Fig.4. All samples display typical IV isotherms with well-defined H1 hysteresis loops (Fig.4a) and characteristic of mesoporous structure. It can be seen that BET surface area of B-OMCs increases with the rise of molar ratio of F/P, so does the microporous volume, which may originate from the volatilization of some small molecules during carbonization. Too excessive formaldehyde will cause much free formaldehyde captured in the cured resins. Furthermore, with the increase of F/P molar ratio, the pore size of the samples increases slightly at first, then decreases from 7.9 nm to 7.0 nm. The larger the molecule is, the more difficult for it to dissolve thoroughly in ethanol, and the more compact the formed micelle will be. Therefore, the pore size of B-OMCs drops step by step.

To quantify the mass fractions of boron in the B-OMC materials, ICP was further employed on obtained B-OMCs (Table 1). With the increase of F/P, boron content of B-OMCs increases distinctly when the molar ratio of F/P reaches 1.5, then decreases slightly. The number of the hydroxymethyl in resol depends on the molar ratio of F/P. Boron is introduced into the backbone of the phenolic resins by boric acid reacting with hydroxymethyl, which is much stable during calcination, while boric acid or other boron compounds are liable to escape above 500 °C. When the molar ratio of F/P is lower, there are not enough hydroxymethyl groups to react with boric acid, so that the boron content of B-OMCs is lower. When the molar ratio of F/P reaches 1.5, boric acid can react with hydroxymetheyl completely to produce BPF with moderate polymerization degree and viscosity. With continuous growth of molar ratio of F/P, poor solubility of BPF in ethanol may not only cause part of BPF molecules inaccessible to the self-assembly procedure, but also interfere with the self-assembly process. Hence, with the molar ratio of F/P reaches 1.5, the boron content of B-OMCs comes to maximum value 1.26 wt%, which is 25% higher than the reported data with same amount of boric acid used (lit.,[23] 1.01 wt%).

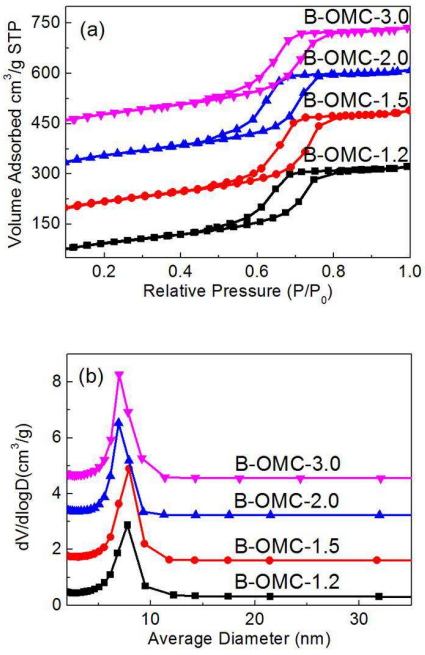

Fig.4 N_2 adsorption-desorption isotherms (a) and pore size distributions (b) of B-OMCs.

In order to further investigate the chemical state of boron and oxygen in the carbon framework, B-OMC-1.5 was selected to conduct X-ray photoelectron spectroscopy (XPS). As shown in Fig.5b, the XPS B1s spectrum for the B-OMC-1.5 can be fitted into three peaks located at 189.8, 191.4 and 192.1 eV, respectively. The B1s with a binding energy of 189.8 eV is assigned to the bonding B-N,[29] which may be formed by reacting

boron with nitrogen during calcination. The boron with B1s at 191.4 eV can be assigned to the mixed B-C and B-O bonding.[18,20] The binding energy of 192.1 eV attributes to the bonding B-O-C,[7] which is consistent with the structure (-O-B-O-C-) generated from trimerization of boric acid, phenol and formaldehyde. In addition, the mass percentage of B in B-OMC-1.5 is 1.48 % (Table 2). The difference of the boron content between ICP and XPS analysis is because most of the boron atoms are not on the surface of mesoporous carbon material for it being bonded chemically to the backbone of B-OMC.

To identify different oxygen species, the O1s spectrum is divided into four peaks attributed to the bonding of C=O (531.8 eV), C-O (532.8 eV), C-OH (533.7 eV) and absorbed water (534.0 eV), respectively.[30] The proportion of oxygen species in B-OMC-1.5 is 31.37 wt% (Table 2), more than twice the result of the literature (lit.,[23] 13.29 wt%). The oxygen groups on the carbon surface are benefit for the capacitance retention at a high scan rate,[16] and can conduct complex faradic reactions with a wide range of beginning potentials and thus enhance the pseudocapacitance.[31] The results suggest that the as-obtained B-OMCs in this work would have a great potential applications in electrochemistry.

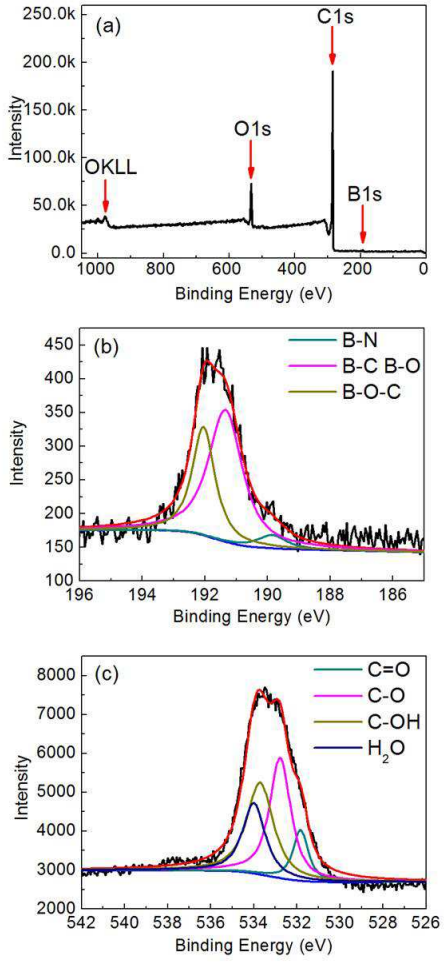

Fig.5 XPS spectra of B-OMC-1.5.

Table 2 XPS results of B-OMC-1.5

Element	B.E. (eV)	Content (wt%)
B	189.8 (B-N)	0.08
	191.4 (B-C/B-O)	0.90
	192.1 (-O-B-O-C-)	0.50
Total content	----	1.48
O	531.8 (C=O)	3.36
	532.8 (C-O)	10.86
	533.7 (C-OH)	10.38
	534.0 (H_2O)	6.77
Total content	----	31.37

The above B-OMCs synthesized under different conditions were subsequently evaluated as the electrodes of supercapacitors. Figure 6 shows the cyclic voltammetry (CV) curves of the B-OMC-x at a scan rate of 5 mV/s, the galvanostatic charge-discharge (GC) profiles at a current density of 0.1 A/g, and the calculated capacitance retention ratios as a function of the current density. The electrochemical performance of the undoped ordered mesoporous carbon (OMC) is also given in Fig.6 for reference. The specific capacitance is 0.18 F/m^2 according to the calculation. As shown in Fig. 6a, all samples present well-symmetric and rectangular CV curves, indicating good electric double layer capacitor (EDLC) performances. It can be seen that the capacitor performance of the B-OMCs as well as their specific capacitance can be substantially improved by introducing boron element. Furthermore, the specific capacitance of a single electrode according to GC test at a current of 0.1 A/g (Fig. 6b) is calculated, and the results are summarized in Table 1. It is found that doping boron will lead to an increase in specific capacitance, from 0.18 F/m^2 (OMC) to 0.27 F/m^2 (B-OMC-1.5). Although this value is still lower than the reported data (lit.,[23] 0.38 F/m^2), the specific capacitance per gram of B-OMC-1.5 is as high as 180 F/g because of its larger specific surface area.

Compared with B-free OMC, boron-doped OMCs caused inferior retention ratio. But as boron content increase, this inferiority exhibited an improved tendency (Fig. 6c). Due to the variation of conductivity and surface hydrophilicity accompanied with boron doped, the kinetic hindrance is strengthened in the transport of both electrons and electrolyte ions. As low B doping influences little on porosities, the variation of retention of B-OMCs with low boron concentration is mainly controlled by the kinetic rather than the diffuse limitation.[23] In general, large amount of B doping would lead to poor ordered mesostructure and small specific surface area, it would be adverse to the diffusion of electrolyte ions and resulting a sharp drop of retention ratio of B-OMCs. However, the B-OMC-1.5, which possesses best-ordered mesostructure, higher specific surface area, larger pore size, has nearly as same retention ratio as undoped OMC, although its boron content is highest .

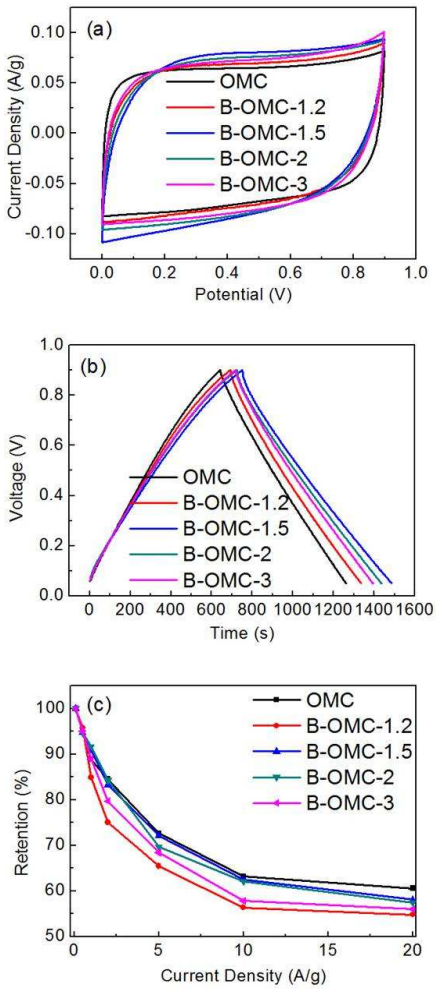

Fig.6 CV curves of B-OMC-x at a scan rate of 5 mV/s (a), GC curves of B-OMC-x at a current density of 0.1 A/g, and capacitance retention as a function of the current density in a 3 M H_2SO_4 electrolyte.

4 Conclusions

A series of B-OMCs were prepared via solvent evaporation induced self-assembly (EISA) method by using boron modified phenolic resins with different molar ratio of F/P as precursors. The results show that the molar ratio of F/P has a significant effect on the mesostructure and boron content of B-OMCs. Along with the increase of molar ratio of F/P, the specific surface area of B-OMCs increases, while pore size and boron content increase first, and then drop off. When the molar ratio of F/P reaches 1.5, the obtained B-OMC have the well-ordered mesoporous structure, higher surface area (667 m^2/g), largest pore size (7.9 nm) and highest boron content (1.26 wt%). Besides, it also possesses excellent electrochemical and capacitance performance (180 F/g).

Acknowledgements

The work was supported by the National Natural Science Foundation of China (51303054), National Key Basic Research Program of China (973 Program) (No. 2013CB035505), Shanghai Leading Academic Discipline Project (B502).

References

1 R. Ryoo, S. H. Joo and S. Jun, *J. Phys. Chem. B*, 1999, **103**, 7743-7746.
2 J. Lee, S. Yoon, T. Hyeon, S. M. Oh and K. B. Kim, *Chem. Commun.*, 1999, 2177-2178.
3 S. H. Joo, S. J. Choi, I. Oh, J. Kwak, Z. Liu, O. Terasaki and R. Ryoo, *Nature*, 2001, **412**, 169-172.
4 A. Stein, Z. Y. Wang and M. A. Fierke, *Adv. Mater.*, 2009, **21**, 265-293.
5 C. Liang, Z. Li and S. Dai, *Angew. Chem. Int. Ed.*, 2008, **47**, 3696-3717.
6 Y. Deng, C. Liu, T. Yu, F. Liu, F. Zhang, Y. Wan, L. Zhang and C. Wang, *Chem. Mater.*, 2007, **19**, 3271-3277.
7 D.-W. Wang, F. Li, Z.-G. Chen, G. Q. Lu and H.-M. Cheng, *Chem. Mater.*, 2008, **20**, 7195-7200.
8 N. Wickramaratne and M. Jaroniec, *RSC Adv.*, 2012, **2**, 1877-1883.
9 Y. Xia and R. Mokaya, *Adv. Mater.*, 2004, **16**, 1553-1558.
10 D. Yuan, X. Yuan, S. Zhou, W. Zou and T. Zhou, *RSC Adv.*, 2012, **2**, 8157-8163.
11 D. Hulicova-Jurcakova, A. M. Puziy, O. I. Poddubnaya, F. Suárez-García, J. M. D. Tascón and G. Q. Lu, *J. Am. Chem. Soc.*, 2009, **131**, 5026-5027.
12 R. Li, Z. Wei, X. Gou and W. Xu, *RSC Adv.*, 2013, **3**, 9978-9984.
13 L. Yang, S. Jiang, Y. Zhao, L. Zhu, S. Chen, X. Wang, Q. Wu, J. Ma, Y. Ma and Z. Hu, *Angew. Chem. Int. Ed.*, 2011, **50**, 7132-7135.
14 Y. Jeong and T. C. M. Chung, *Carbon*, 2010, **48**, 2526-2537.
15 Y. Shao, X. Wang, M. Engelhard, C. Wang, S. Dai, J. Liu, Z. Yang and Y. Lin, *J. Power Sources*, 2010, **195**, 4375-4379.
16 X. Zhao, A. Wang, J. Yan, G. Sun, L. Sun and T. Zhang, *Chem. Mater.*, 2010, **22**, 5463-5473.
17 Y. Hishiyama, H. Irumano, Y. Kaburagi and Y. Soneda, *Phys. Rev. B*, 2001, **63**, 245406.
18 D. H. Zhong, H. Sano, Y. Uchiyama and K. Kobayashi, *Carbon*, 2000, **38**, 1199-1206.
19 S. Shiraishi, M. Kibe, T. Yokoyama, H. Kurihara, N. Patel, A. Oya, Y. Kaburagi and Y. Hishiyama, *Appl. Phys. A: Mater. Sci. Process.*, 2006, **82**, 585-591.
20 S. Ding, S. Zheng, M. Xie, L. Peng, X. Guo and W. Ding, *Microporous. Mesoporous. Mater.*, 2011, **142**, 609-613.
21 X. Zhai, Y. Song, J. Liu, P. Li, M. Zhong, C. Ma, H. Wang and Q. Guo, *J. Electrochem. Soc.*, 2012, **159**, E177-E182.
22 X. Zhai, Y. Song, L. Zhi, Y. Shi and Q. Guo, *New Carbon Mater.*, 2011, **26**, 211-216.
23 X. Zhao, Q. Zhang, B. Zhang, C.-M. Chen, J. Xu, A. Wang, D.-S. Su and T. Zhang, *RSC Adv.*, 2013, **3**, 3578-3584.
24 Y. Meng, D. Gu, F. Zhang, Y. Shi, H. Yang, Z. Li, C. Yu, B. Tu and D. Zhao, *Angew. Chem. Int. Ed.*, 2005, **44**, 7053-7059.
25 P. P. Chu and H.-D. Wu, *Polymer*, 2000, **41**, 101-109.
26 Y. Meng, D. Gu, F. Zhang, Y. Shi, L. Cheng, D. Feng, Z. Wu and Z. Chen, *Chem. Mater.*, 2006, **18**, 4447-4464.
27 J. Gao, X. Su and L. Xia, *Int. J. Polym. Mater.*, 2005, **54**, 949-961.
28 Y. Du, F. Ji, Z. Liu and C. Lv, *Polymer Materials Science & Engineering*, 2003, **19**, 44-47.
29 T. Sugino and S. Tagawa, *Appl. Phys. Lett.*, 1999, **74**, 889-891.
30 S. D. Gardner, C. S. K. Singamsetty, G. L. Booth, G.-R. He and C. U. Pittman Jr, *Carbon*, 1995, **33**, 587-595.
31 T. Kwon, H. Nishihara, H. Itoi, Q.-H. Yang and T. Kyotani, *Langmuir*, 2009, **25**, 11961-11968.